

## Structural evolution of carbon nanotubes in composites under contact sliding stresses

I. Zarudi and L. C. Zhang<sup>a)</sup>

School of Aerospace, Mechanical and Mechatronic Engineering, The University of Sydney, Building J07, New South Wales 2006, Australia

(Received 22 November 2005; accepted 15 May 2006; published online 12 June 2006)

We discovered a new structural evolution of carbon nanotubes (CNTs) in epoxy composites subjected to contact sliding stresses. Our analysis under high resolution transmission electron microscopy showed that the evolution has three stages which are (a) the bonding breakage of the CNTs, (b) the formation of sinusoidal shells, and (c) the consolidation of nanoparticles. We then explored the evolution mechanisms theoretically. © 2006 American Institute of Physics.

[DOI: 10.1063/1.2212063]

Deformation of carbon nanotubes (CNTs), including those in composites, has attained extensive research attention.<sup>1–5</sup> For example, Marques *et al.*<sup>1</sup> considered the performance of CNTs under tension and showed that the brittle or plastic response under high stretching conditions is controlled by the rate of straining and number of defects in a nanotube. Wagner *et al.*<sup>2</sup> studied the fragmentation of CNTs in polymer composites under tension and compression. They concluded that the fragmentation was due to either (1) compressive thermal residual stresses resulting from polymer shrinkage during polymerization or (2) tensile stresses generated by polymer deformation and transmitted to CNTs during testing.

It was demonstrated that during the deformation of CNTs by ball milling<sup>4</sup> a high percentage of CNTs had partially or completely collapsed openings. Also an incident of carbon nanoparticles was reported after 10–15 min of high speed milling.<sup>6</sup>

This letter studies the deformation and structural transformation of CNTs in an epoxy composite when subjected to contact sliding stresses (wear tests). The deformation mechanism revealed by our study was never discovered before, but it is critical to the tribological behavior of composites reinforced by CNTs.

The multiwalled CNTs used in our experiment were prepared by chemical vapor deposition (provided by Nanolab) with diameters ranging from 10 to 20 nm and lengths varying from 10 to 20  $\mu\text{m}$ .

Dry wear tests were carried out on a Plint-Cameron pin-on-disk machine,<sup>7</sup> on which two pin samples were held against a rotating high speed steel disk of hardness  $H_{\text{MV}}=720$ . A fixed track diameter of 80 mm was used in all the tests with a sliding distance of 2500 m, normal nominal stress of 1 MPa, and sliding velocity of 0.98 m/s.

Conventional transmission electron microscopy (TEM) studies were performed in a Philips CM12 transmission electron microscope, operating at 120 kV. The high-resolution transmission electron microscopy (HRTEM) investigations were performed on a JEOL JEM-3000F transmission electron microscope, operating at 300 kV.

TEM specimens were prepared in the standard manner using a tripod. To ensure that no changes of epoxy microstructure would take place during its exposure to acetone, a sample's surface was covered with thin amorphous chromium film that was completely removed at the last stage of the sample's preparation. Plan view samples were prepared with the thinning procedure performed from the side opposite to wear surface.

The general view of CNTs in the epoxy CNT-reinforced composite before contact sliding is presented in Fig. 1(a). The diameters and lengths of the CNTs are 10–25 nm and 2–5  $\mu\text{m}$ , respectively, having a bamboo conical structure. The microstructure of the CNT-reinforced epoxy after a wear test is presented in Fig. 1(b). It is obvious that most of the CNTs are fragmented to segments of 100–400 nm. The CNT walls are no longer smooth and with atomic distortion and

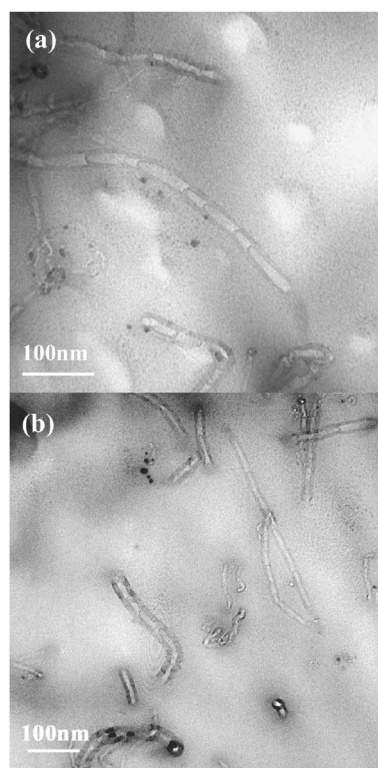


FIG. 1. CNTs in composite. (a) before wear test and (b) after wear test.

<sup>a)</sup> Author to whom correspondence should be addressed; electronic mail: zhang@aeromech.usyd.edu.au

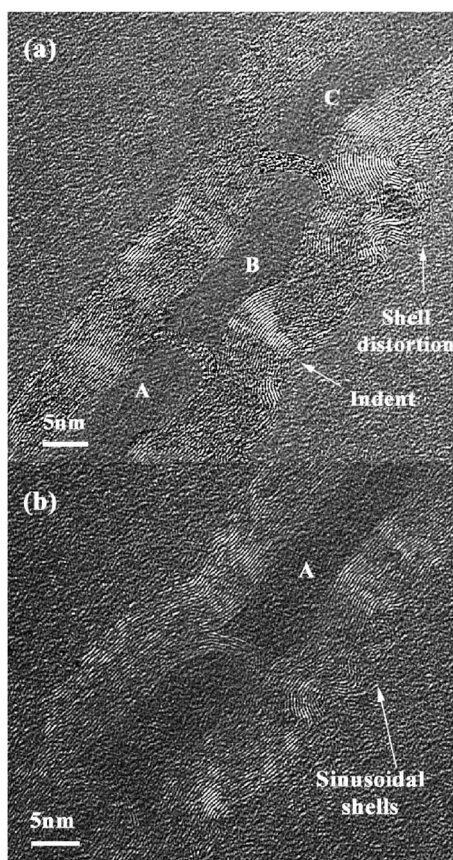


FIG. 2. HRTEM deformation of the bamboo CNTs after wear test: (a) zones A–C. Note an indentation of the outer wall by the disk asperity that leads to the distortion of the CNT walls to its whole depth. (b) Zone A in more detail. Note the sinusoidal shape of the outer shells.

dislocations, Figs. 2(a) and 2(b). These types of permanent deformation of the walls due to the repeated interaction of composite with the steel disk surface in contact sliding of the wear test led to the outer shell breakages of the CNTs.

We discovered several very interesting deformation mechanisms of CNTs. Figure 2(a) shows zones A–C of a bamboo CNT structure. Zone A [Fig. 2(b)] features a sinusoidal distortion of six carbon outer shells. Zone B presents an altered CNT wall with another type of deformation [Fig. 2(b)]. The carbon shells deform to the whole depth of CNT walls and have nearly semicircular shapes. It seems that the pattern can be the result of indentation of a sharp asperity into the outer shell perpendicular to the CNTs' axis. The same type of deformation occurs in zone C. The above deformation mechanisms have never been reported. In contact sliding the composite is interacting with asperities of steel disk. These asperities can act as sharp indenters that deform CNT walls. Asperities can also cause tensile deformation as CNTs are fixed in epoxy matrix and can be stretched. For example, about six outer shells were stretched in zone A, forming a sinusoidal shape on stress release. Surprisingly, even after heavy deformation, no gaps were detected between CNTs and epoxy matrix. It seems that the adhesion and stress transfer ability between CNTs and epoxy are strong.<sup>8</sup> Also, elevated temperatures arising in a wear test could possibly softened the epoxy, but the high strain rate in the test could make it harder at the elevated level.<sup>9</sup>

CNTs with open and closed ends were detected after the wear tests. Those with closed ends were not altered by con-

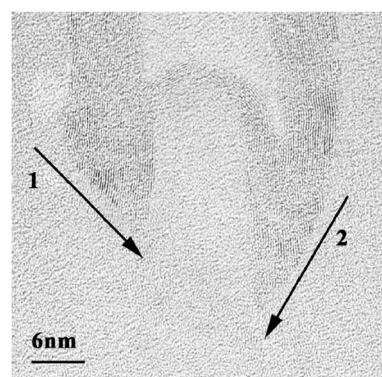


FIG. 3. HRTEM of the CNTs with an open end. Note the breakage of the left wall and imperfection in the microstructure of the right wall (breakage steps are indicated by arrows).

tact sliding. However, CNTs with open ends (Fig. 3) were generated during wear. (The CNTs were tilted inside TEM, which confirmed the observation.) An open end of the CNT is asymmetric with one side 5 nm longer than the other (Fig. 3), indicating that breakage did not take place perpendicular to the CNT's axis but at an inclined angle. The other feature of the end is its partial imperfection of the right wall, demonstrating that the breakage of the CNT could be the result of the multiple asperity-CNT interactions. Directions of breakage can be seen in Fig. 3, indicated by the arrows.

More interestingly, nanoparticles were found in the composite after the wear tests. These nanoparticles were similar to those obtained by electron irradiation<sup>10</sup> or ball milling<sup>6</sup> and were of two main kinds. Some of them has faceted or partly faceted walls [Fig. 4(a)]. These nanoparticles had an inner diameter of 5–8 nm and a moderate number of shells (about 15–18). Another kind of nanoparticles has spherical shapes, resembling an onionlike structure [Fig. 4(b)], which is clearly different from those reported by Ugarte *et al.*,<sup>10</sup>

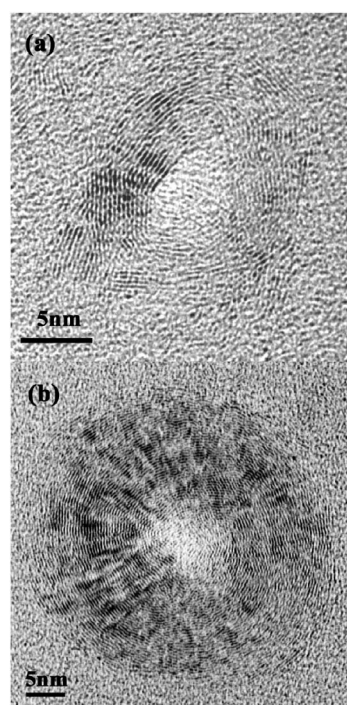


FIG. 4. HRTEM images of nanoparticles on the sample's surface after wear test; (a) a faceted nanoparticle and (b) an onionlike nanoparticle.

TABLE I. Data on the asperities of the steel disk and composite.

	rms ( $\mu\text{m}$ )	Standard deviation of the heights distribution ( $\mu\text{m}$ )	Asperity's density ( $\text{asp}/\mu\text{m}^2$ )	Average asperity's radius ( $\mu\text{m}$ )
The steel disk	0.6	0.3	0.15	0.5
The composite before wear test	0.08	0.05	0.02	0.03
The composite after wear test	0.03	0.015	$8 \times 10^4$	0.007

because in the present case, the inner core of a nanoparticle is amorphous with a diameter of 4–5 nm and the particle shells have a large number of defects. In addition, the outer and inner shells are not continuous. As concluded by Iijima,<sup>11</sup> the onionlike nanoparticles are the most stable. An irradiation treatment transforms metastable faceted nanoparticles to more stable circular onionlike particles,<sup>10</sup> because the system under irradiation is stabilized by the energy gain from the van der Waals interaction between shells.<sup>12</sup> In our present case, an irradiation source does not exist and hence the transformation from the faceted to the onionlike structure must have been due to the deformation caused by sliding stresses. It seems to indicate that sharp corners between facets might have acted as stress concentrators during composite-disk interaction and were removed first. Meanwhile, mechanical deformation also destroys some shells leading to many defects in the inner structure of the nanoparticles.

To estimate the actual contact stresses caused by the steel disk asperities, the surface topographies of the disk and composite were measured, as listed in Table I. We assume that the deformation of the sliding system consists of the following two stages.<sup>13</sup> Stage 1, microscale deformation occurs in the steel disk only; no changes take place in the composite material. Stage 2, nanoscale deformation takes place in the composite, while the steel disk in stage 1 keeps its deformed topography unchanged.

The Greenwood-Williamson statistical model<sup>14</sup> can then be applied to these two stages individually. The first deals with the deformation of the steel disk that gives rise to the load ( $P_1$ ) on each asperity of the steel disk. In the second stage each asperity of the steel disk interacts with the nanoasperities (the CNTs) on the composite surface with load  $P_1$  (see Ref. 13 for details). By applying the Greenwood-Williamson model again, the load on each CNT,  $P_2$ , is determined.

Since the surface roughness of the composite (rms=0.08  $\mu\text{m}$ ) is much less than that of the steel disk (rms=0.6  $\mu\text{m}$ ), its surface is considered to be smooth in our stage 1 analysis. The average pressure on each steel disk asperity was found as  $P_1 = P / \pi \eta A \beta \sigma F_1(h)$ , where  $P$  is a load on a whole sliding surface,  $\pi = 3.14$ ,  $\eta$  is a surface density of asperities,  $A$  is a nominal contact area,  $\beta$  is an asperity radius,  $\sigma$  is a standard deviation of asperities height distribution,  $h$  is a standard separation, and  $F_1(h) = (1/\sqrt{2\pi}) \int_1^\infty (s-h)e^{-0.5s^2} ds$ .  $P_1$  was calculated to be 0.76 GPa. On stage 2 the similar analysis gave an average pressure on CNTs to be 8.36 GPa.

According to Shen and Jiang,<sup>15</sup> a pressure of 5.3 GPa is enough to break the ends of a CNT in sliding motion. It is clear that the pressure of 8.36 GPa applied in our wear tests is above this threshold and that was why the CNT caps were removed. This enables the formation of sinusoidal shells, and consequently leads to the consolidation of nanoparticles.

We have revealed a new structural evolution of CNTs in epoxy composites during contact sliding and have shown that the evolution has three stages which are (a) the bonding breakage of the CNTs, (b) the formation of sinusoidal shells, and (c) the consolidation of nanoparticles. The first stage is critical and the sliding stress must be high enough to enable the evolution to occur.

The authors wish to thank the Australian Research Council (ARC) for continuing support of this project and the Electron Microscope Unit of Sydney University for the use of its facilities.

<sup>1</sup>M. A. L. Marques, H. E. Troiani, M. Miki-Yoshida, M. Jose-Yacamán, and A. Rubio, *Nano Lett.* **4**, 811 (2004).

<sup>2</sup>H. D. Wagner, O. Lourie, and X. F. Zhou, *Composites, Part A* **30**, 59 (1999).

<sup>3</sup>C. A. Cooper, S. R. Cohen, A. H. Barber, and H. D. Wagner, *Appl. Phys. Lett.* **81**, 3873 (2002).

<sup>4</sup>Z. Konya, J. Zhu, K. Niesz, D. Mehn, and I. Kiricsi, *Carbon* **42**, 2001 (2004).

<sup>5</sup>K. Mylvaganam and L. C. Zhang, *Nanotechnology* **17**, 410 (2006).

<sup>6</sup>Y. B. Li, B. Q. Wei, J. Liang, Q. Yu, and D. H. Wu, *Carbon* **37**, 493 (1999).

<sup>7</sup>L. C. Zhang, I. Zarudi, and K. Q. Xiao, *Wear* (in press).

<sup>8</sup>K. Q. Xiao and L. C. Zhang, *J. Mater. Sci.* **39**, 4481 (2004).

<sup>9</sup>W. D. Cook, A. E. Mayr, and G. H. Edward, *Polymer* **39**, 3725 (1998).

<sup>10</sup>D. Ugarte, *Carbon* **33**, 989 (1995).

<sup>11</sup>S. Iijima, *J. Cryst. Growth* **50**, 675 (1980).

<sup>12</sup>D. Ugarte, *Europhys. Lett.* **22**, 45 (1993).

<sup>13</sup>L. C. Zhang and I. Zarudi, *Wear* **229**, 669 (1999).

<sup>14</sup>J. A. Greenwood and J. B. P. Williamson, *Proc. R. Soc. London, Ser. A* **295**, 300 (1966).

<sup>15</sup>W. Shen and B. Jiang, *Phys. Rev. Lett.* **84**, 3634 (2000).